The effect of speed and influence of individual muscles on hamstring mechanics during the swing phase of sprinting

Elizabeth S. Chumanov[a], Bryan C. Heiderscheit[b,c], Darryl G. Thelen[a,b,c],*

[a]*Department of Mechanical Engineering, University of Wisconsin-Madison, 1513 University Ave., Madison, WI 53706, USA*
[b]*Department of Biomedical Engineering, University of Wisconsin-Madison, 1550 Engineering Drive, Madison, WI 53706, USA*
[c]*Department of Orthopedics and Rehabilitation, University of Wisconsin-Madison, Madison, WI 53706, USA*

Abstract

The purpose of this study was to characterize the effect of speed and influence of individual muscles on hamstring stretch, loading, and work during the swing phase of sprinting. We measured three-dimensional kinematics and electromyography (EMG) activities of 19 athletes sprinting on a treadmill at speeds ranging from 80% to 100% of maximum speed. We then generated muscle-actuated forward dynamic simulations of swing and double float phases of the sprinting gait cycle. Simulated lower extremity joint angles and model predicted excitations were similar to measured quantities. Swing phase simulations were used to characterize the effects of speed on the peak stretch, maximum force, and negative work of the biceps femoris long head (BF), the most often injured hamstring muscle. Perturbations of the double float simulations were used to assess the influence of individual muscles on BF stretch.

Peak hamstring musculotendon stretch occurred at ~90% of the gait cycle (late swing) and was independent of speed. Peak hamstring force and negative musculotendon work increased significantly with speed ($p < 0.05$). Muscles in the lumbo-pelvic region had greater influence on hamstring stretch than muscles acting about the knee and ankle. In particular, the hip flexors were found to induce substantial hamstring stretch in the opposite limb, with that influence increasing with running speed. We conclude that hamstring strain injury during sprinting may be related to the performance of large amounts of negative work over repeated strides and/or resulting from a perturbation in pelvic muscle coordination that induces excessive hamstring stretch in a single stride.

1. Introduction

Acute hamstring strain injuries are commonly linked with maximal speed running in a variety of sports such as track, football and soccer (Gabbe et al., 2005; Woods et al., 2004). While it is generally agreed that strain injuries are the result of exceeding the local mechanical limits of the muscle tissue, little is known on how running speed changes the mechanical demands of the hamstrings. Such information is relevant for establishing a scientific basis for injury prevention programs and rehabilitative approaches that can mitigate the high risk for re-injury (Orchard and Best, 2002). For example, a recent study found that the performance of rehabilitative exercises targeting neuro-muscular control of muscles in the lumbo-pelvic region (e.g. abdominal obliques, erector spinae, illiopsoas) reduced hamstring re-injury rates compared to a stretching and strengthening approach (Sherry and Best, 2004). However, the complexities of multi-segmental dynamics (Zajac and Gordon, 1989) make it challenging to understand how lumbo-pelvic muscles may influence hamstring mechanics, and hence injury risk.

Prior studies have shown that the biarticular hamstrings are active (Jonhagen et al., 1996; Swanson and Caldwell, 2000; Wood, 1987) and undergo a stretch-shortening cycle (Thelen et al., 2005a) during the second half of the swing phase of sprinting. The hamstrings do a substantial amount of negative work over this period, with the peak stretch of the hamstring musculotendon unit occurring during late

*Corresponding author. Tel.: +1 608 262 1902; fax: +1 608 265 2316.
E-mail address: thelen@engr.wisc.edu (D.G. Thelen).

swing (Thelen et al., 2005b; van Don, 1998; Wood, 1987). Thus, the hamstrings are likely susceptible to a lengthening contraction injury during late swing. We have previously shown that peak musculotendon stretch is invariant as speed increases from submaximal to maximal speeds (Thelen et al., 2005b). The purpose of this study was to utilize simulations of subject-specific sprinting dynamics to test the hypothesis that sprinting speed increases the loading and negative work required of the hamstrings. We also evaluated the sensitivity of hamstring stretch to perturbations in individual muscle forces, to understand the potential influence that lumbo-pelvic muscles have on injury risk.

2. Methods

2.1. Subjects

19 athletes participated in this study (Table 1). All subjects had experience sprinting on a treadmill. Testing was conducted at two sites: the Orthopedic Specialty Hospital in Murray, UT and the University of Wisconsin-Madison in Madison, WI. The testing protocol was approved

Table 1
Subject characteristics and maximum treadmill sprinting speed ($V_{\max}$) of the athletes who participated in this study

	Mean (s.d.)	
	Males	Females
Number of subjects	14	5
Age (yr)	20.9 (5.7)	19.6 (6.4)
Height (cm)	179 (8)	176 (5)
Body mass (kg)	78.6 (9.6)	65.7 (4.2)
$V_{\max}$ (m/s)	9.10 (0.60)	8.18 (0.77)

by the Institutional Review Boards at both institutions and all subjects provided informed consent in accordance with institutional policies.

2.2. Experimental protocol

Whole body kinematics were recorded using 40 reflective markers placed on each subject, with 21 located on anatomical landmarks. In addition, a subset ($n = 5$) of the subjects had electromyography (EMG) surface electrodes placed on muscles of the right lower limb: biceps femoris (BF), medial hamstrings (ST and SM), vastus lateralis, rectus femoris, and the medial gastrocnemius. After the markers and EMG electrodes were in place, each subject warmed up prior to sprinting at 80%, 85%, 90%, 95%, and 100% of his/her maximum speed, with 5 strides (3–5 s) collected for each trial. Subjects were given adequate rest between trials. A standing trial was also performed to establish segment lengths, joint centers and joint coordinate systems.

2.3. Data acquisition

Three-dimensional kinematics were collected at 200 Hz using an 8-camera passive marker system (Motion Analysis Corporation, Santa Rosa, CA). Kinematics data were low pass filtered using a bi-directional, 4th order Butterworth filter with a cutoff frequency of 12 Hz. Foot contact times were ascertained from a contact-induced vertical acceleration of the 5th metatarsal toe marker at foot strike. The validity of this approach was verified with pressure sensitive foot switches on four of the subjects.

EMG activities were recorded (synchronously with kinematics at 2000 Hz) using single differential, surface electrodes with an inter-electrode distance of 10 mm (DE-2.1, DelSys, Inc., Boston, MA). Each electrode pre-amplified the signal and interfaced to an amplifier unit (Bagnoli-16, DelSys, Boston, MA). The EMG signals were subsequently full-wave rectified and low pass filtered using a bi-directional, 6th order Butterworth filter with a cutoff frequency of 20 Hz.

2.4. Musculoskeletal model

The body was modeled as a 14 segment, 31 degree of freedom (DOF) articulated linkage (Fig. 1). Anthropometric properties of the segments were scaled to each individual using the subject's height, mass and segment
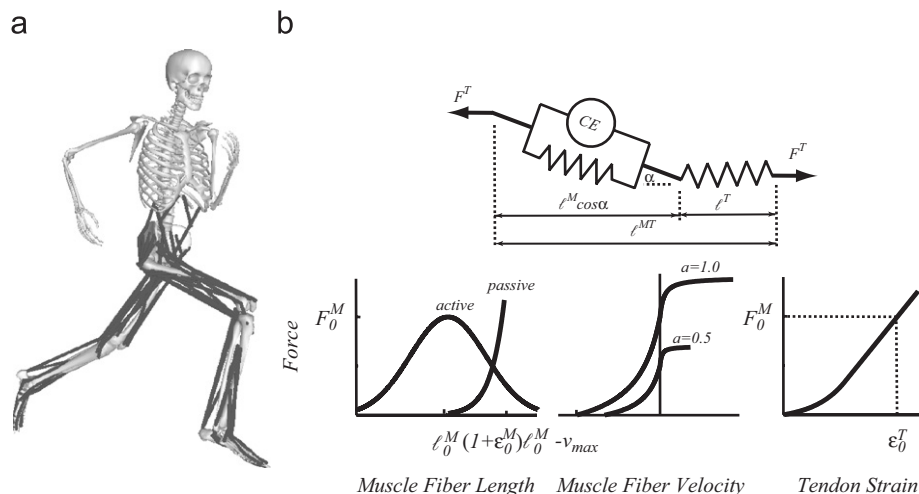

Fig. 1. (a) A forward dynamic musculoskeletal model, shown with 92 musculotendon actuators, was used to simulate both the swing phase and double float phases of sprinting. (b) A Hill-type model was used to characterize musculotendon contraction dynamics. The muscle force–length–velocity properties and tendon force–strain properties were scaled to each muscle using four parameters: ℓ_0^M—optimal fiber length, F_0^M—maximum isometric force, ℓ_s^T—tendon slack length and α_0—fiber pennation angle (Zajac, 1989). Parameters used for the biarticular hamstring muscles were adapted from the literature (Delp et al., 1990; Arnold, et al., 2000) (1) BF: $\ell_0^M = 0.109$ m, $\ell_s^T = 0.341$ m, $F_0^M = 1792$ N, $\alpha_0^M = 0°$, (2) ST: $\ell_0^M = 0.201$ m, $\ell_s^T = 0.262$ m, $F_0^M = 820$ N, $\alpha_0^M = 5°$, SM: $\ell_0^M = 0.08$ m, $\ell_s^T = 0.359$ m, $F_0^M = 2576$ N, $\alpha_0^M = 15°$.

lengths (de Leva, 1996). Each hip was modeled as a ball and socket joint with three DOF. The knee was represented as a one DOF joint, in which the tibiofemoral translations and nonsagittal rotations were constrained functions of knee flexion–extension angle (Walker et al., 1988). The ankle–subtalar complex was represented by two revolute joints aligned with anatomical axes (Delp et al., 1990). The low back was represented as a ball and socket joint at the 3rd lumbar vertebra (Anderson and Pandy, 1999). For each trial, joint angles were computed at each time step using a global optimization routine to minimize the sum of squared error between the measured and model marker positions (Lu and O'Connor, 1999).

Musculotendon actuators were represented as line segments connecting the origin to the insertion with wrapping about joints and other structures accounted for with wrapping surfaces (Arnold et al., 2000). The input to each musculotendon actuator was an idealized excitation level that varied between zero and one (full excitation). Muscle excitation-to-activation dynamics was represented using a first-order differential equation that had a faster time constant during activation (10 ms) than deactivation (30 ms). A Hill-type model (Fig. 1) of musculotendon contraction dynamics was assumed, where muscle fibers were in series with an elastic tendon (Zajac, 1989). Force produced by the musculotendon actuator was applied to the segments to which it attached. The equations of motion of the musculoskeletal model were derived using SDFast (Parametric Technology Corporation, Waltham, MA) and SIMM Pipeline (Musculographics Inc., Chicago, IL).

2.5. Forward dynamic simulations

We generated muscle-actuated forward dynamic simulations of swing limb movement to characterize hamstring stretch, force and work. In *swing phase* simulations, 52 musculotendon actuators (26 actuators on each limb) were used to actuate 3 DOF on each limb (hip flexion–extension, hip adduction–abduction, knee flexion–extension). All other DOF were prescribed to follow the measured kinematics trajectories, thereby accounting for inter-segmental dynamics. Swing phase simulations were generated for 3 strides for each subject at each speed.

We also generated forward dynamic simulations of the *double float phase* of sprinting (i.e. when both feet are off the ground) to assess the influence of individual muscles on hamstring stretch. Double float phase was selected because peak hamstring musculotendon stretch occurs during this time period. In the double float simulations, 92 musculotendon actuators (43 on each limb and 6 acting about the low back) were used to actuate 21 DOF (6 DOF for the pelvis and each limb, 3 DOF about the low back), with only the upper extremity DOF prescribed to follow measured trajectories. Double float phase simulations were generated for one stride at 80% and 100% speeds for 4 subjects, for whom we had a full set of kinematics, EMG and foot switch data.

A computed muscle control (CMC) algorithm was used to determine muscle excitation patterns that, when input into the forward dynamic

model, produced joint angles that closely replicated experimental kinematics. A brief description of the CMC algorithm follows (for details, see Thelen and Anderson, 2006). When computing the excitations, we first determined the difference between the experimental and simulated joint angles and angular velocities. These errors were fed back and combined with the experimental accelerations to compute a set of desired accelerations to ensure that the experimental kinematics were tracked. We then determined a set of muscle excitations that would generate the desired accelerations, while minimizing a cost function (sum of muscle volume-weighted squared activations, Happee, 1994) to resolve muscle redundancy. Computed muscle excitations were then input into the forward dynamic model equations, which were numerically integrated to generate a set of simulated muscle excitations, activations, lengths, musculotendon forces and joint kinematics. The excitations were re-computed using this process at 0.01 s intervals throughout the simulations.

Swing phase simulations, in which muscles actuated 3 DOF on each limb, were used to characterize the musculotendon stretch, force and power development of the biarticular hamstrings. Stretch was defined as the change in length of the musculotendon unit relative to the relaxed length in an upright posture. Relaxed lengths were estimated by setting all joint angles and muscle excitations to zero in the subject-specific scaled model. The musculotendon power generated (absorbed) was computed as the product of the force and musculotendon velocity. Negative and positive musculotendon work was computed by integrating the respective portions of the power curves. A one-way repeated measures analysis of variance was used to determine the effects of normalized speed (80%, 85%, 90%, 95%, and 100%) on the magnitude of peak musculotendon stretch, force, and negative work. Tukey's post hoc test was used to analyze significant main effects. The statistical analyses were completed using Systat (SPSS Inc., Chicago, IL) with a significance level of 0.05.

Perturbations of the *double float phase* simulations, in which muscles actuated 21 DOF, were performed to investigate how individual muscles influence BF musculotendon stretch (Fig. 2). We report perturbation results for the BF because it is the most frequently injured of the hamstring muscles (Connell et al., 2004); the perturbation results for the other biarticular hamstrings were similar. For each muscle in the model, the nominal force trajectory was perturbed by a fixed ratio (0.1%) throughout double float, while the excitations of all other muscles were held constant (Fig. 2). The musculoskeletal dynamic model equations were then re-integrated to produce a perturbed set of joint and musculotendon kinematic trajectories. It is noted that perturbation-induced changes in kinematics could alter the lengths and velocities, and hence forces, of other muscles in the system, thereby reflecting the complex interactions inherent in the musculoskeletal system (Goldberg et al., 2004). The influence of an individual muscle was then defined as the change in the peak stretch of the BF scaled by the inverse of the force perturbation magnitude. Perturbations with a fixed force magnitude (1 N) were also performed to assess the potential of muscles to influence biceps femoris stretch per unit force (Goldberg et al., 2004).
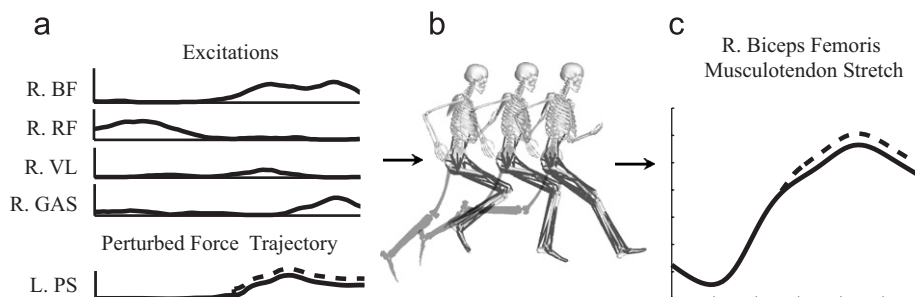

Fig. 2. In the perturbation analyses used to assess muscle influence, we first generated forward dynamic simulations of the double float phase of sprinting in which all lower extremity and low back degrees of freedom were actuated by muscles (note that left limb muscles are not shown for clarity). (a) We then perturbed individual muscle force trajectories, one at a time, by 0.1% throughout the simulation while other muscle excitations were held constant (solid line is nominal trajectory, dashed line is perturbed force trajectory). (b) The movement was then re-simulated. (c) The difference in the BF nominal length (solid line) and perturbed length (dashed line) was attributed to the force perturbation. The change in peak musculotendon stretch was scaled by the inverse of the perturbation magnitude to determine the absolute influence of the muscle on BF stretch.

3. Results

The CMC algorithm generated simulations that closely tracked the experimental kinematics (Fig. 3). For the swing phase simulations, RMS errors for the hip and knee angles were $1.0 \pm 0.7°$ for hip flexion–extension, $0.7 \pm 0.3°$ for hip abduction–adduction, and $2.2 \pm 1.2°$ for knee flexion–extension. For the double float simulations, the average RMS errors for the actuated 21 DOF were $3.3 \pm 4.3°$. The simulated muscle excitation patterns of the lower limb muscles were similar to measured EMG signals (Fig. 4). Hamstring muscle excitations were initiated at $\sim 70\%$ of the gait cycle and remained elevated throughout the remainder of swing phase. The hamstring musculotendon units lengthened from approximately 50–90% of the gait cycle with peak force reached between 85% and 95% of the gait cycle (Fig. 5).

Peak hamstring musculotendon stretch was independent of speed. However, both peak musculotendon force and negative musculotendon work increased significantly ($p < 0.01$) with speed (Fig. 6). The average peak net hamstring force increased from 36 N/kg at the 80% speed to 52 N/kg at maximal speed, while the average net negative work increased from 1.4 to 2.6 J/kg (Table 2).

The influence of individual muscles on hamstring stretch was larger at maximal speed when compared to slower speeds (Fig. 7). Other than the hamstrings themselves, muscles in the lumbo-pelvic region had the greatest
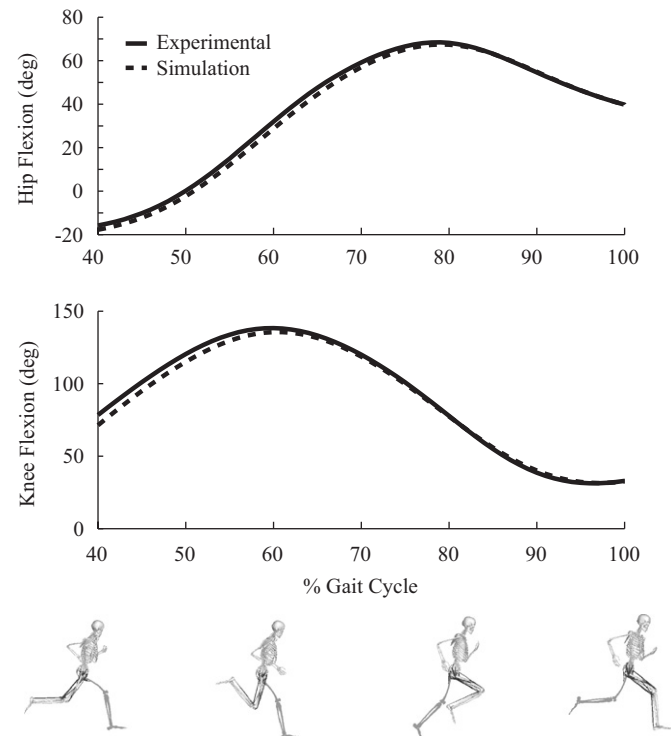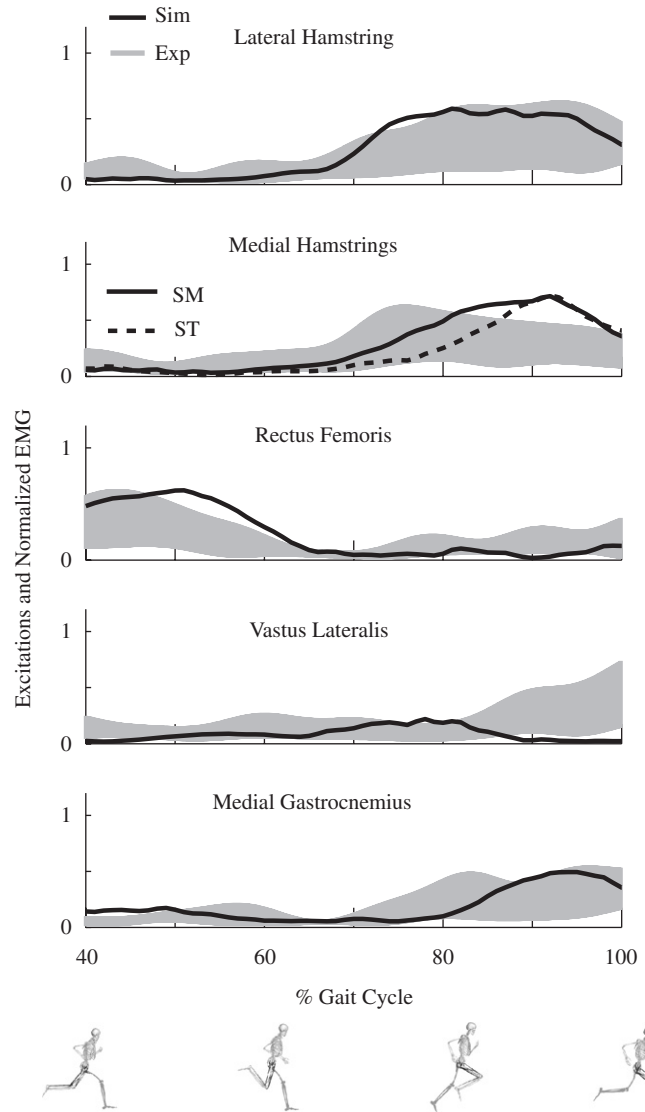
Fig. 4. The timing of simulated muscle excitations (solid lines) and measured electromyographic (EMG) activities (shaded curves) were relatively consistent for the hamstrings, rectus femoris and gastrocnemius muscles. Vastus excitations during late swing are presumably in preparation for the subsequent stance phase, which was not simulated. Simulated excitations are the ensemble average of the predicted excitations across all subjects at the maximum sprinting speed. EMG activities are the mean (± 1 s.d.) rectified, low-pass filtered activities recorded from five subjects at maximal speed.

Fig. 3. A sample swing phase simulation is shown demonstrating that the simulated hip and knee angles closely tracked the experimentally quantities.

influence (Fig. 7) and potential influence (Fig. 8) on hamstring stretch. These muscles included the uniarticular hip flexors (iliopsoas), the gluteus maximus, the erector spinae and the internal and external obliques. The right adductor magnus has a large potential influence (Fig. 8) to decrease BF stretch, resulting from it's substantial hip extension moment arm when the hip is flexed (Delp et al., 1990). However, the actual influence of adductor magnus was substantially less because the muscle was not predicted to be active during double float. At the maximum speed, the uniarticular hip flexors induced > 20 mm increase in BF stretch on the opposite limb, which was of comparable
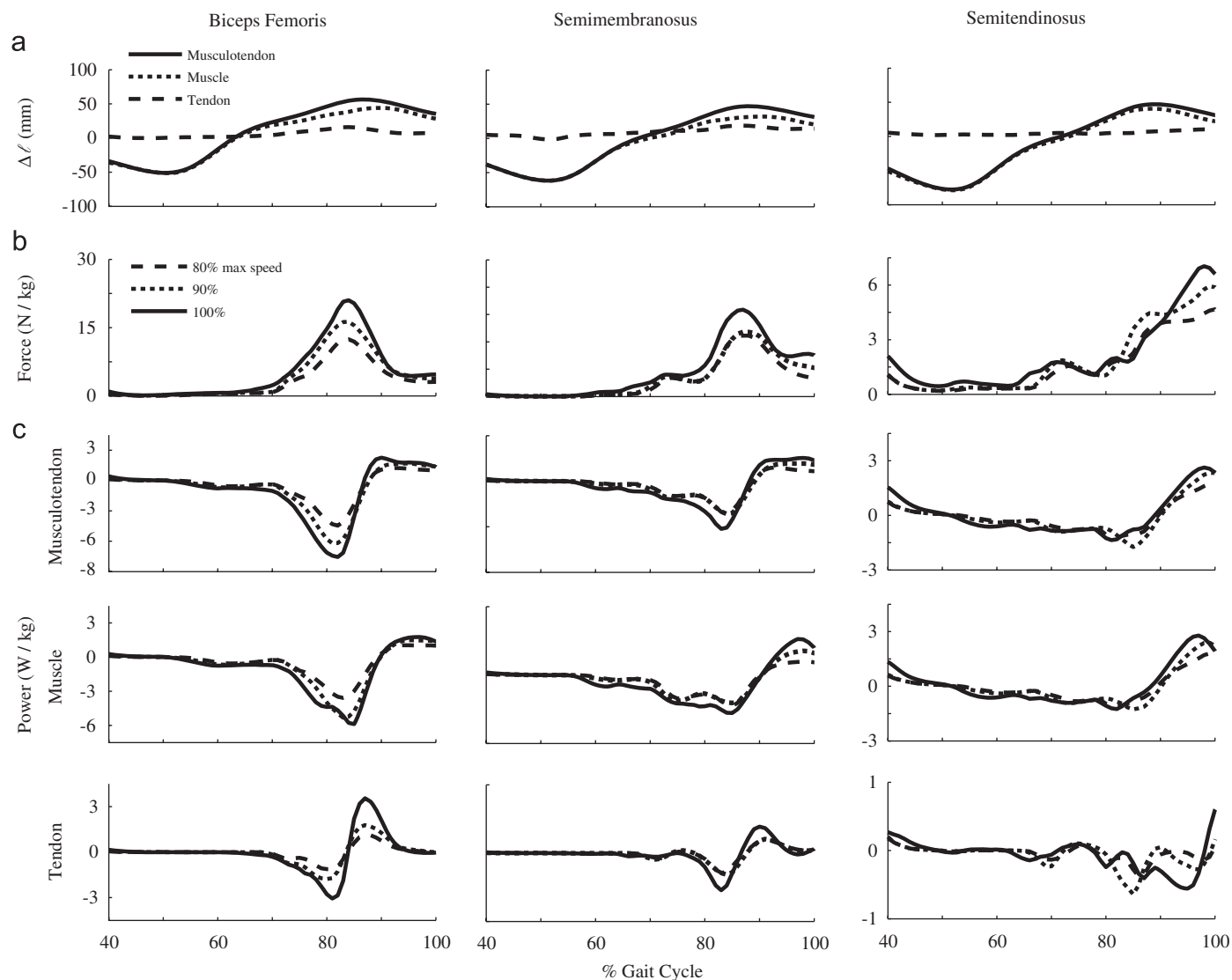
Fig. 5. Simulated musculotendon mechanics of the hamstring muscles for one subject. (a) The change in length (Δl) from a relaxed, upright posture of the musculotendon, muscle component and tendon at maximal sprinting speed. The musculotendon stretches more than the muscle component during late swing due to the tendon stretching as force develops (Thelen, et al., 2005a). (b) Musculotendon forces increase with speed for each of the hamstring muscles, with peak forces occurring slightly earlier in the biceps femoris and semimembranosus, compared to the semitendinosus. (c) The hamstring musculotendon units do a considerable amount of negative work up until the final 10% of the gait cycle.

magnitude to the decrease in stretch induced by the hamstrings themselves.

4. Discussion

In this study, we used forward dynamic simulations of sprinting to investigate changes in hamstring mechanics with speed. The salient findings were that speed significantly increases the amount of negative work the hamstrings do, and magnifies the influence that individual muscles, particularly the muscles in the lumbo-pelvic region, have on hamstring stretch.

Previous studies investigating joint mechanics (Kuitunen et al., 2002; Mann, 1981; Swanson and Caldwell, 2000) and muscle activation patterns (Jonhagen et al., 1996; Mero

and Komi, 1987) during sprinting have shown that coupled hip extensor and knee flexor moments are utilized during the late swing phase of sprinting (Kuitunen et al., 2002), presumably to decelerate the limb prior to foot contact. EMG data indicate that the medial and lateral biarticular hamstrings exhibit peak activities during late swing, and increase significantly with speed (Mero and Komi, 1987). The modeling approach used in this study extends these results, by providing quantitative predictions of the mechanical loading of the hamstrings during this period.

We found that the peak musculotendon stretch of the hamstrings does not vary significantly across speeds ranging from 80% to 100% of maximum, which is consistent with our results on a smaller group of subjects (Thelen et al., 2005b). Joint kinematic patterns have been

shown to be relatively consistent across a range of sprinting speeds (Thelen et al., 2005b), suggesting the primary speed effect is an increase in the rate at which the joint angular excursions are traversed. Therefore, the energy associated with the limb would be expected to increase in proportion to the joint angular velocities, and equivalently sprinting speed, squared. Such a relationship is evident in Fig. 6, where the negative musculotendon work increases at a faster rate than peak musculotendon force.

Animal models of muscle injury have provided insights into the relationship between mechanical measures and the degree of injury. In animal models, the best indicators of injury potential are the magnitude of strain (Brooks and Faulkner, 2001; Lieber and Friden, 1993; Lieber and Friden, 2002), or the product of force and strain (Brooks and Faulkner, 2001), which may in effect be equivalent measures for maximally activated muscle (Brooks et al.,
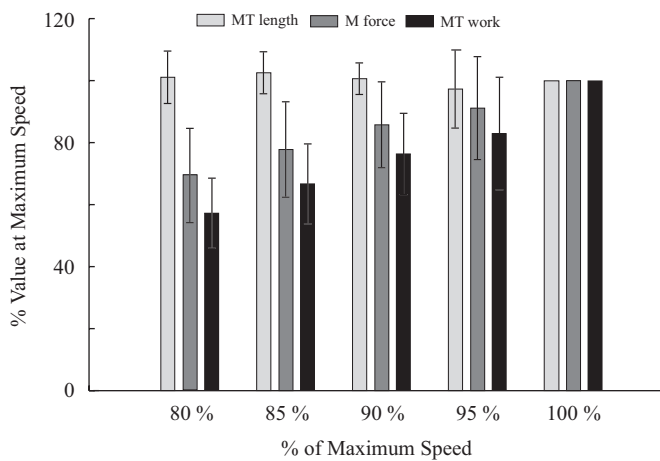

Fig. 6. The relative (compared to 100% or maximal speed) biceps femoris musculotendon stretch, negative work, and force. Peak musculotendon stretch is invariant with sprinting speed, while force and negative work increase significantly with speed. Negative musculotendon work increased to the largest extent as sprinting speed was increased from submaximal to maximal sprinting speeds.
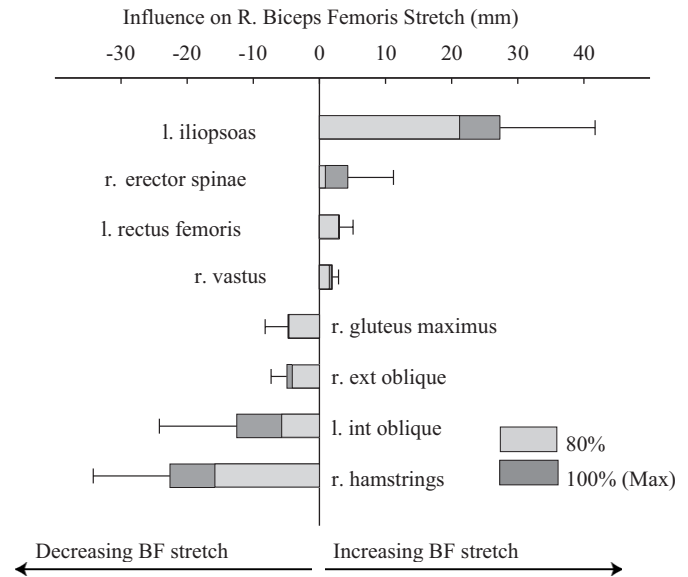

Fig. 7. The muscles that had the greatest magnitude of influence on biceps femoris stretch during double float are shown. Note that the influence of each muscle increased as speed was increased from submaximal to maximal, reflecting the larger forces present at high speeds. When the hamstring muscles are given a positive perturbation, the hamstring force increases and contributes to a decrease in peak stretch. In contrast, the uniarticular hip flexors (iliopsoas) are simultaneously active on the opposite limb inducing a substantial increase in biceps femoris stretch.

Table 2
Mean (s.d.) kinematic and kinetic measures from the hamstring muscles across all subjects. Relative to the length in a relaxed upright posture, the biceps femoris (BF) exhibited greater musculotendon stretch than the semimembranosus (SM) and semitendinosus (ST). Both the force developed and negative musculotendon work done by the hamstrings increased significantly with sprinting speed (Δl^{MT} = peak musculotendon stretch, F_{max} = peak muscle force per unit body mass, W_{neg}^{MT} = negative work done by the musculotendon unit per unit body mass)

Measure	Speed (% max)	BF		SM		ST		NET	
Δl^{MT} (mm)	80	51.4	(5.6)	43.5	(5.1)	44.7	(5.5)		
	85	52.2	(4.8)	44.1	(4.6)	45.1	(5.2)		
	90	51.4	(4.3)	42.8	(4.0)	43.4	(4.4)		
	95	49.9	(7.9)	41.2	(8.6)	41.3	(10.4)		
	100	51.2	(4.4)	42.6	(4.6)	42.9	(5.4)		
F_{max} (N/kg)[a]	80	15.1	(6.3)	18.9	(6.2)	6.4	(1.3)	36.0	(12.4)
	85	16.8	(6.4)	21.4	(6.9)	6.7	(1.2)	40.5	(13.8)
	90	18.6	(6.8)	23.3	(8.6)	7.1	(1.3)	45.2	(15.4)
	95	19.8	(7.0)	25.7	(9.7)	7.4	(1.4)	49.2	(16.1)
	100	21.4	(5.4)	27.9	(7.6)	7.9	(1.8)	52.0	(13.4)
W_{neg}^{MT} (J/kg)[a]	80	0.47	(0.23)	0.50	(0.26)	0.21	(0.06)	1.40	(0.62)
	85	0.53	(0.26)	0.59	(0.31)	0.23	(0.08)	1.65	(0.73)
	90	0.61	(0.31)	0.69	(0.37)	0.25	(0.10)	1.92	(0.88)
	95	0.65	(0.31)	0.79	(0.42)	0.27	(0.13)	2.23	(0.97)
	100	0.77	(0.28)	0.99	(0.44)	0.35	(0.18)	2.61	(1.01)

[a]Significant speed effects.

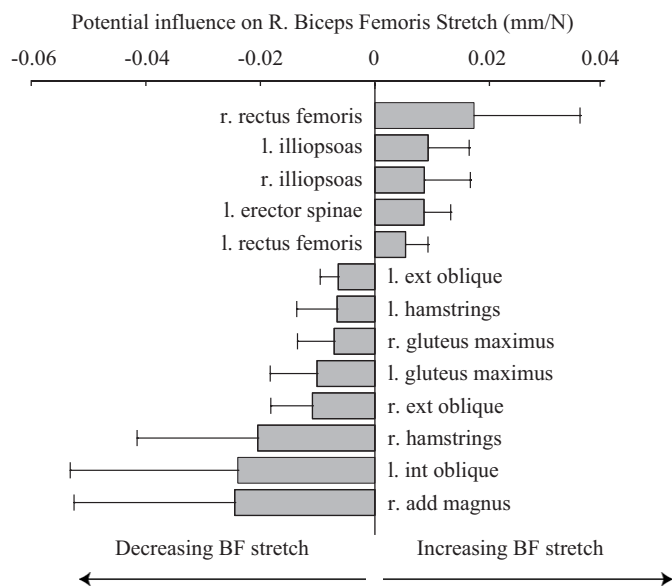Potential influence on R. Biceps Femoris Stretch (mm/N)

Fig. 8. Muscles in the lumbo-pelvic region have the largest potential to influence biceps femoris stretch during double float phase. Muscles not shown (including the vasti, gastrocnemius, soleus, tibialis anterior, gluteus medius and gluteus minimus) exhibited average potential influences that were less than 0.005 mm/N.

1995). In this study, which involves variable activation levels, we have shown differential effects of sprinting speed on musculotendon stretch (comparable to mechanical strain) and negative work.

Our results indicate two, potentially inter-related, factors contributing to increased injury risk at high speed. One possibility is a large amount of negative work done over repeated strides may result in accumulated microdamage that predisposes the muscle to injury. This would be consistent with a recent animal model of injury, which showed that multiple stretch-shortening contractions are needed to induce injury when muscle lengths are constrained to physiological ranges (Butterfield and Herzog, 2005). Secondly, fluctuations in neuromuscular control at high speed could create stride-to-stride variability in hamstring stretch, with excessive stretch in any single stride inducing an acute onset of injury. These factors could also be inter-related with microdamage due to multiple stretch-shortening cycles altering musculotendon properties, thus changing the threshold for injury over time (Butterfield and Herzog, 2005), making an individual more susceptible to stride-to-stride variations in hamstring stretch.

Our perturbation analyses suggest a mechanism by which a rehabilitation program focused on core neuromuscular training (Sherry and Best, 2004) could influence hamstring re-injury risk. We showed that muscles in the lumbo-pelvic regions have substantial influence on the overall stretch of the BF. For example, activation of the uniarticular hip flexors (iliopsoas) during early swing induces stretch of the hamstrings on the opposite limb. This coupling arises due to inter-segmental dynamics, in

which muscles can generate substantial accelerations about joints they do not span (Zajac and Gordon, 1989). In our simulations, the hip flexor muscle force induced hip flexion and a small amount of knee extension on the opposite limb which both act to increase hamstring stretch. The magnitude of this increased stretch was comparable to the shortening induced by the hamstrings themselves, demonstrating the importance of considering inter-segmental dynamics.

There are a number of assumptions in the musculotendon models that should be considered when interpreting the results. First while we scaled the lengths and moment arms of the musculotendon unit based on subject-specific segment lengths, we relied on literature-derived estimates for other important parameters such as maximum isometric force, optimum fiber length, and tendon compliance. As a result, there is a degree of uncertainty in the absolute accuracy of our force, length and work measures. For example, we have previously demonstrated that tendon compliance has substantial affects on fiber stretch and negative work done by the muscle component (Thelen et al., 2005a). For this reason, we limited our dependence on model parameters by only considering speed-dependent changes in musculotendon measures (rather than muscle and tendon component measures) to evaluate our primary hypotheses. New imaging techniques to empirically characterize in vivo musculotendon mechanics (Fukunaga et al., 2002) may facilitate more detailed subject-specific models that are needed to enhance the accuracy of model predictions at the muscle and tendon level. Our analyses were also limited to swing phase where peak hamstring stretch occurs. However, muscle activations during stance also influence kinematics during swing (Goldberg et al., 2004), and should be considered to fully understand the influence of individual muscles on injury risk.

In conclusion, our results support the idea that acute hamstring strain injury may be related to performance of large amounts of negative work over repeated strides and/ or changes in neuromuscular coordination that induce excessive stretch of the hamstrings.

Conflict of interest

There is no conflict of interest.

Acknowledgments

References

Anderson, F.C., Pandy, M.G., 1999. A dynamic optimization solution for vertical jumping in three dimensions. Computer Methods in Biomechanics and Biomedical Engineering 2, 201–231.

Arnold, A.S., Salinas, S., Asakawa, D.J., Delp, S.L., 2000. Accuracy of muscle moment arms estimated from MRI-based musculoskeletal models of the lower extremity. Computer Aided Surgery 5, 108–119.

Brooks, S.V., Faulkner, J.A., 2001. Severity of contraction-induced injury is affected by velocity only during stretches of large strain. Journal of Applied Physiology 91, 661–666.

Brooks, S.V., Zerba, E., Faulkner, J.A., 1995. Injury to muscle fibres after single stretches of passive and maximally stimulated muscles in mice. Journal of Physiology 488, 459–469.

Butterfield, T.A., Herzog, W., 2005. Quantification of muscle fiber strain during in vivo repetitive stretch-shortening cycles. Journal of Applied Physiology 99, 593–602.

Connell, D.A., Schneider-Kolsky, M.E., Hoving, J.L., Malara, F., Buchbinder, R., Koulouris, G., Burke, F., Bass, C., 2004. Longitudinal study comparing sonographic and MRI assessments of acute and healing hamstring injuries. American Journal of Roentgenology 183, 975–984.

de Leva, P., 1996. Adjustments to Zatsiorsky–Seluyanov's segment inertia parameters. Journal of Biomechanics 29, 1223–1230.

Delp, S.L., Loan, J.P., Hoy, M.G., Zajac, F.E., Topp, E.L., Rosen, J.M., 1990. An interactive graphics-based model of the lower extremity to study orthopaedic surgical procedures. IEEE Transactions on Biomedical Engineering 37, 757–767.

Fukunaga, T., Kawakami, Y., Kubo, K., Kanehisa, H., 2002. Muscle and tendon interaction during human movements. Exercise Sport Science Reviews 30, 106–110.

Gabbe, B.J., Finch, C.F., Bennel, K.L., Wajswelner, H., 2005. Risk factors for hamstring injuries in community level Australian football. British Journal of Sports Medicine 39, 106–110.

Goldberg, S.R., Anderson, F.C., Pandy, M.G., Delp, S.L., 2004. Muscles that influence knee flexion velocity in double support: implications for stiff-knee gait. Journal of Biomechanics 37, 1189–1196.

Happee, R., 1994. Inverse dynamic optimization including muscular dynamics, a new simulation method applied to goal directed movements. Journal of Biomechanics 27, 953–960.

Jonhagen, S., Ericson, M.O., Nemeth, G., Eriksoon, E., 1996. Amplitude and timing of electromyographic activity during sprinting. Scandinavian Journal of Medicine and Science in Sports 6, 15–21.

Kuitunen, S., Komi, P.V., Kyrolainen, H., 2002. Knee and ankle joint stiffness in sprint running. Medicine and Science in Sports and Exercise 34, 166–173.

Lieber, R.L., Friden, J., 1993. Muscle damage is not a function of muscle force but active muscle strain. Journal of Applied Physiology 74, 520–526.

Lieber, R.L., Friden, J., 2002. Mechanisms of muscle injury gleaned from animal models. American Journal of Physical Medicine and Rehabilitation 81, S70–S79.

Lu, T.W., O'Connor, J.J., 1999. Bone position estimation from skin marker co-ordinates using global optimisation with joint constraints. Journal of Biomechanics 32, 129–134.

Mann, R.V., 1981. A kinetic analysis of sprinting. Medicine and Science in Sports and Exercise 13, 325–328.

Mero, A., Komi, P.V., 1987. Electromyographic activity in sprinting at speeds ranging from sub-maximal to supra-maximal. Medicine and Science in Sports and Exercise 19, 266–274.

Orchard, J., Best, T.M., 2002. The management of muscle strain injuries: an early return versus the risk of recurrence. Clinical Journal of Sport Medicine 12, 3–5.

Sherry, M., Best, T., 2004. A comparison of two rehabilitation programs in the treatment of acute hamstring strains. Journal of Orthopaedic and Sports Physical Therapy 34, 116–125.

Swanson, S., Caldwell, G., 2000. An integrated biomechanical analysis of high speed incline and level treadmill running. Medicine and Science in Sports and Exercise 32, 1146–1155.

Thelen, D.G., Anderson, F.C., 2006. Using computed muscle control to generate forward dynamic simulations of human walking from experimental data. Journal of Biomechanics 39, 1107–1115.

Thelen, D.G., Chumanov, E.S., Best, T.M., Swanson, S.C., Heiderscheit, B.C., 2005a. Simulation of biceps femoris musculotendon mechanics during the swing phase of sprinting. Medicine and Science in Sports and Exercise 37, 1931–1938.

Thelen, D.G., Chumanov, E.S., Hoerth, D.M., Best, T.M., Swanson, S.C., Li, L., Young, M., Heiderscheit, B.C., 2005b. Hamstring muscle kinematics during treadmill sprinting. Medicine and Science in Sports and Exercise 37, 108–114.

van Don, B.J., 1998. Hamstring injuries in sprinting. Ph.D. Dissertation, The University of Iowa.

Walker, P.S., Rovick, J.S., Robertson, D.D., 1988. The effects of knee brace hinge design and placement on joint mechanics. Journal of Biomechanics 21, 965–974.

Wood, G., 1987. Biomechanical limitations to sprint running. Medicine and Science in Sports and Exercise 25, 58–71.

Woods, C., Hawkins, R.D., Maltby, S., Hulse, M., Thomas, A., Hodson, A., 2004. The football association medical research programme: an audit of injuries in professional football—analysis of hamstring injuries. British Journal of Sports Medicine 38, 36–41.

Zajac, F.E., 1989. Muscle and tendon: properties, models, scaling and application to biomechanics and motor control. Critical Reviews in Biomedical Engineering 17, 359–411.

Zajac, F.E., Gordon, M.E., 1989. Determining muscle's force and action in multi-articular movement. Exercise and Sport Sciences Reviews 17, 187–230.